

# 1 DeLTA 3.0: A modern segmentation and tracking tool 2 for microscopy images

3 **Virgile Andreani**  <sup>1,2</sup>¶, **Jean-Baptiste Lugagne**  <sup>1,3</sup>, **Owen M. O'Connor**  <sup>1</sup>,  
4 **Mary J. Dunlop**  ¶

5 **1** Biomedical Engineering, Boston University, USA **2** EPI Lifeware, Inria Saclay, France **3** Department of  
6 Engineering Science, University of Oxford, United Kingdom ¶ Corresponding author

DOI: [10.xxxxxx/draft](https://doi.org/10.xxxxxx/draft)

## Software

- 7 ▪ [Review](#) ↗
- [Repository](#) ↗
- [Archive](#) ↗

Editor: ↗

Submitted: 10 October 2025

Published: unpublished

## License

Authors of papers retain copyright  
and release the work under a  
Creative Commons Attribution 4.0  
International License ([CC BY 4.0](#))

## Summary

8 Time-lapse microscopy is a popular and widely used approach for quantifying single-cell  
9 dynamics. Analysis of sequences of images requires two steps: segmentation—locating the cells  
10 in each frame—and tracking—identifying how cells in one frame relate to the next. DeLTA  
11 (Deep Learning for Time-lapse Analysis) is a Python ([Perez et al., 2011](#)) package that performs  
12 segmentation and tracking. It was initially developed to handle images of bacteria growing  
13 within the “mother machine,” ([Wang et al., 2010](#)) a popular microfluidic device for single-cell  
14 analysis that constrains cells to grow in one dimension ([Lugagne et al., 2020](#)), and was later  
15 extended to handle cells growing in two dimensions ([O'Connor et al., 2022](#)). After three years  
16 of experience and feedback from our group and the broader community, we are releasing version  
17 3.0—a major overhaul designed to achieve four key objectives: enhance usability for scientists,  
18 improve modularity and adaptability for developers, integrate common features like growth rate  
19 computation and lineage manipulation, and adopt modern open-source development practices.

## Statement of need

21 DeLTA is a deep learning pipeline for analysing bacterial time-lapse microscopy images.

22 This third version adds functionalities while remaining true to DeLTA’s principles. DeLTA  
23 distinguishes itself from other packages by:

- 24 ▪ the simplicity of its implementation, making its code pedagogical and easily adaptable;
- 25 ▪ its built-in handling of mother machine settings, a widely-used device where segmentation  
26 and tracking are performed within several regions of interest on each frame;
- 27 ▪ its ability to cater to novice and experienced users alike, respectively through a new  
28 interface allowing users to run and train DeLTA without writing code, and through an  
29 API allowing programmatic and real-time use;
- 30 ▪ new utilities provided for common analysis functions (e.g., robust estimation of growth  
31 rate, correcting tracking errors).

32 In addition, in this version, deep learning models have been ported to keras ([Chollet & Others,](#)  
33 [2015](#)), a high-level backend-agnostic library that allows users to select any of the three main  
34 deep learning backends (tensorflow ([Abadi et al., 2015](#)), torch ([Ansel et al., 2024](#)), or jax  
35 ([Bradbury et al., 2018](#))).

## State of the field

36 When DeLTA was originally developed, only CellProfiler ([Stirling et al., 2021](#)) and DeepCell  
37 ([Valen et al., 2016](#)) existed in the Python ecosystem for cell segmentation and tracking

39 using deep learning. Since then, several other tools have been developed, including Cellpose  
40 ([Stringer et al., 2021](#)), Omnipose ([Cutler et al., 2022](#)), MM3 ([Thiermann et al., 2024](#)) and  
41 Cell-TRACTR ([O'Connor & Dunlop, 2025](#)). DeLTA's first version was developed around the  
42 mother machine. To date, only DeLTA and MM3 offer built-in mother machine support. The  
43 second version of DeLTA extended analysis to two-dimensional growth, further expanding the  
44 utility of the software. The current version makes it the only package to provide robust growth  
45 rate estimation and utilities to manipulate lineages and fix tracking errors.

## 46 Software Design

47 DeLTA's design philosophy is based on a trade-off around four principles: (1) user-friendly  
48 defaults and interfaces to empower less-technical users, (2) a modular API to allow expert  
49 users to address all situations, (3) minimizing custom code when reliable and performant  
50 libraries exist, and (4) providing reliable utilities for the most common needs of users beyond  
51 pure segmentation and tracking.

52 Version 3 aims to improve all four principles:

- 53 1. The command-line interface that this version introduces enables the use of DeLTA  
54 without writing code for segmentation, tracking, and model training.
- 55 2. The API has been rationalized to reduce naming and usage inconsistencies.
- 56 3. We adopted an open data model, based on xarray (in memory) and netCDF4 (for file  
57 storage), to replace our custom pickle-based object serialization, to allow any third-party  
58 package to open DeLTA result files. Details and trade-offs related to this approach are  
59 described in [section 9](#).
- 60 4. We provided two utilities to address exceedingly common needs of experimentalists: the  
61 computation of instantaneous cell growth rate, and an interface to fix tracking errors.  
62 See [section 8](#) and [section 7](#) for details on the implementations of these features.

## 63 Research Impact Statement

64 As one of the first packages using deep learning for the segmentation and tracking of single  
65 cells, DeLTA has had a significant research impact ([Ahmadi et al., 2024](#); [Allard et al., 2022](#);  
66 [Gericke et al., 2025](#)) and is an inspiration or comparison point for the development of other  
67 packages ([O'Connor & Dunlop, 2025](#); [Thiermann et al., 2024](#)).

68 DeLTA is widely used by researchers internationally. The articles describing earlier versions  
69 have accumulated a total of >350 citations to date.

70 Currently, DeLTA is downloaded ~220 times per month on PyPI and ~430 times per month on  
71 conda-forge.

<sup>72</sup> General principles of the package

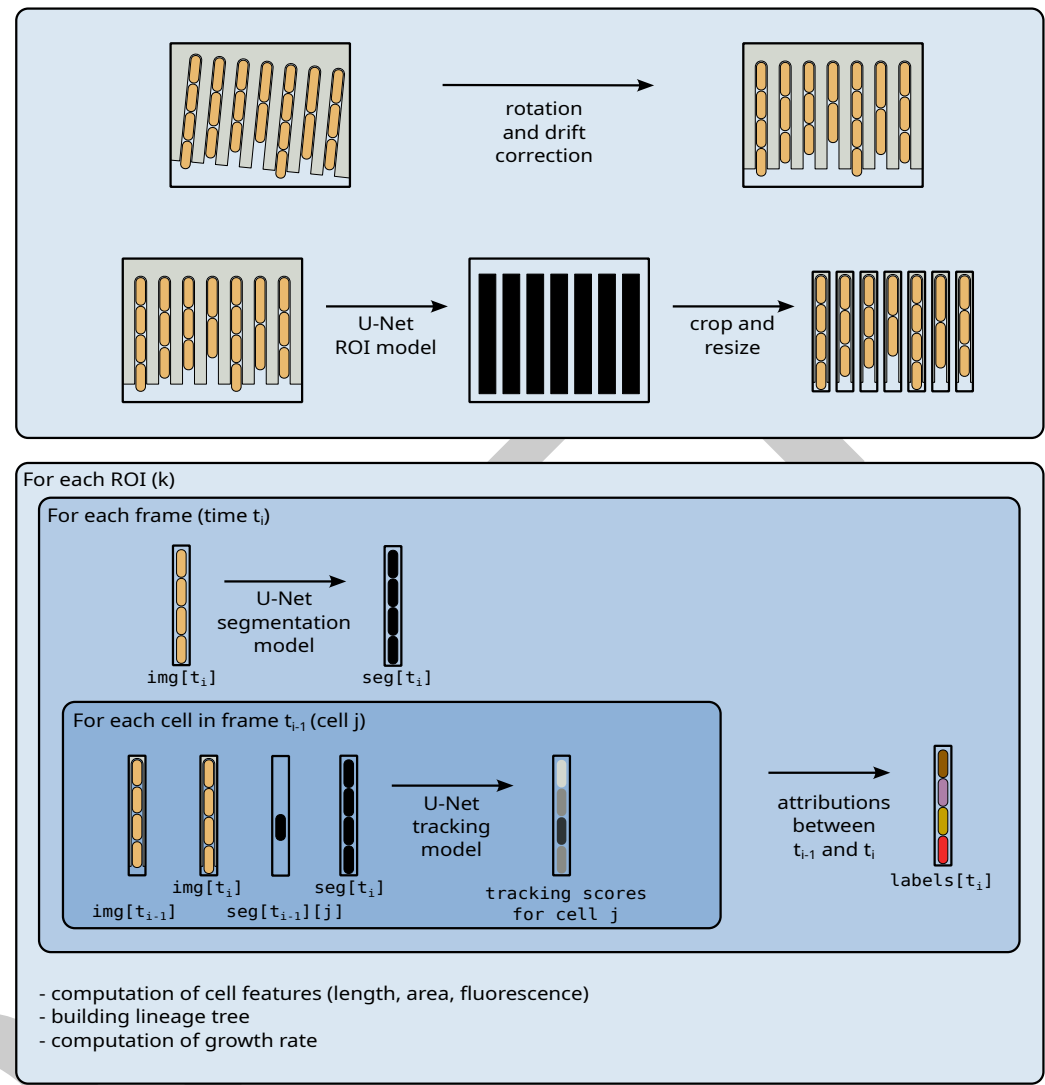


**Figure 1:** Schematic principles of DeLTA. First, any rotation and drift are removed from the movie. Then, in the case of a mother machine experiment, a region of interest (ROI) model detects and crops individual chambers. Then, for each ROI, each frame is segmented with a U-Net, and passed to a tracking model with the previous frame and the mask of a single cell in the previous frame, to generate tracking scores that determine attribution. Finally, morphological cell features are computed, the lineage tree is built, and growth rates are computed.

<sup>73</sup> DeLTA uses three different U-Net ([Ronneberger et al., 2015](#)) models: for region of interest  
<sup>74</sup> (ROI) identification, segmentation, and tracking. Once ROIs have been identified and resized,  
<sup>75</sup> the segmentation model is run frame-by-frame to determine the location of cells. Finally, for  
<sup>76</sup> every consecutive pair of frames, the tracking model is run once per cell in the earlier frame,  
<sup>77</sup> to determine the probabilities that this cell corresponds to each cell in the later frame. After  
<sup>78</sup> mother-daughter relationships have been determined, a lineage tree is constructed [[section 7](#)]  
<sup>79</sup> where cell features are stored: area, length, average fluorescence, and growth rate [[section 8](#)].  
<sup>80</sup> Finally, these results are saved as a netCDF file accompanied by a segmented movie for direct  
<sup>81</sup> visualization.

82 **Lineage**

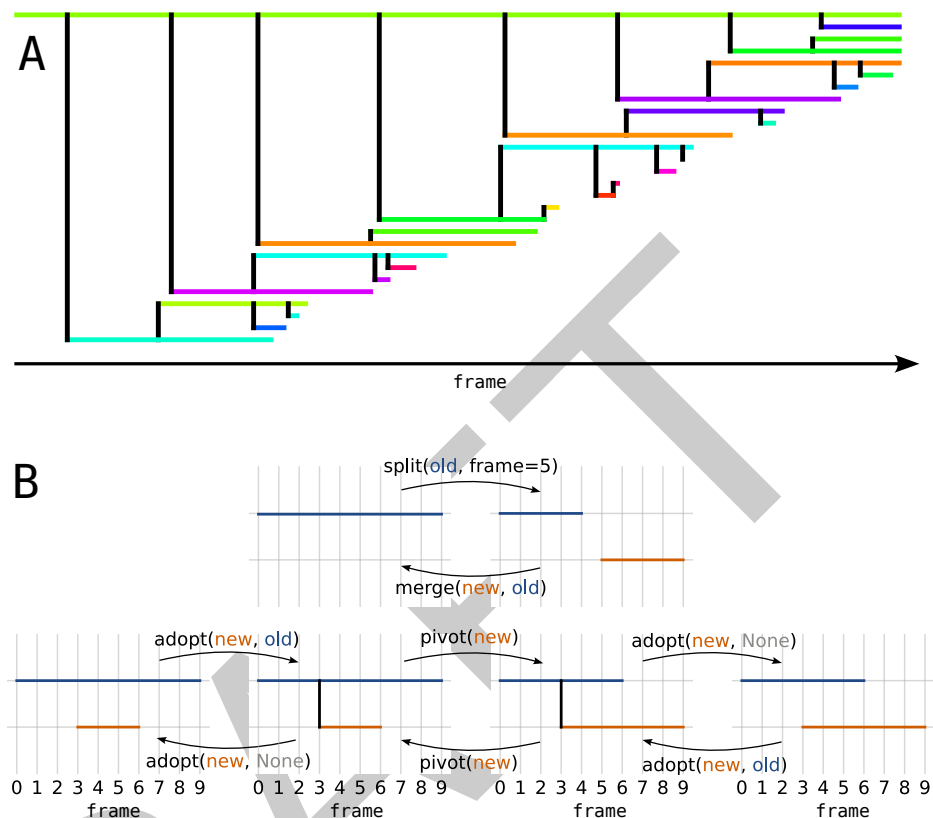
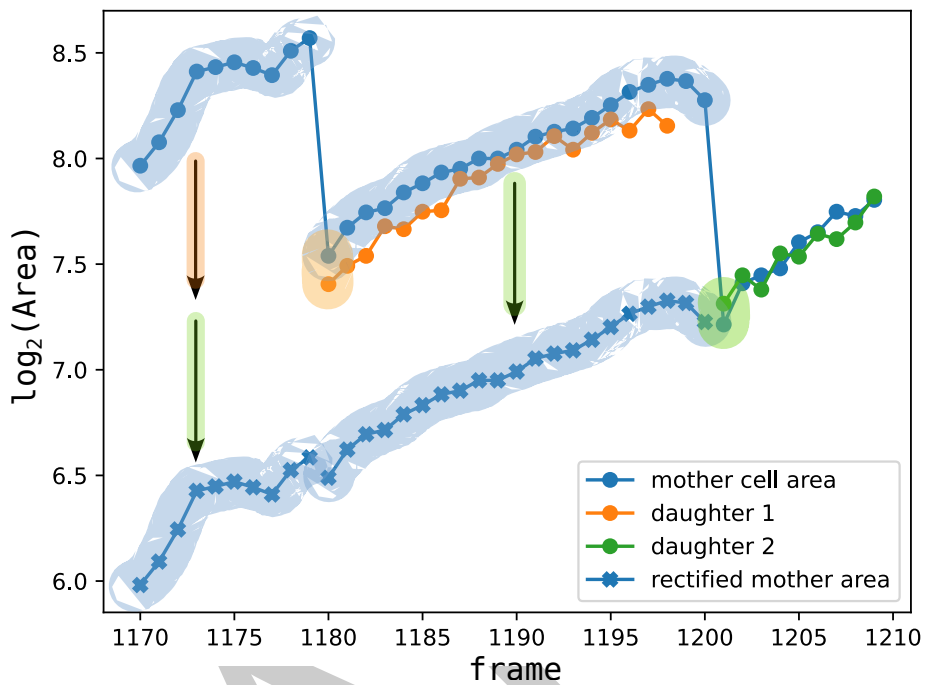


Figure 2: Lineage tree manipulation. **A:** Lineage tree of one chamber from a mother machine experiment. Horizontal lines represent individual cells, while vertical black lines represent division events. Cells exit at the bottom of the mother machine, so some lineages terminate before the end of the figure. The top “mother” cell is trapped and remains in the mother machine throughout the full time range. **B:** This set of functions can be used to correct any tracking errors. If DeLTA fails to associate one cell with itself in the next frame, the merge function can be used to mend the line. The split function does the opposite. The adopt function can set or unset a mother-daughter relationship, while pivot switches a mother and a daughter (the mother being by convention the cell with the oldest pole).

83 The tracking functionality of DeLTA detects cell divisions, linking mother cells to their daughters.  
 84 Bacterial cell divisions are typically symmetrical, however pole age has measurable effects on  
 85 cell physiology, where the daughter cell that inherits the older end of the mother cell grows  
 86 more slowly than the other daughter (Stewart et al., 2005). For this reason, we consider that  
 87 the mother cell persists through divisions, giving birth to one daughter (instead of the mother  
 88 cell disappearing and giving rise to two daughter cells). Thus, upon cell division, the mother  
 89 cell retains its ID number, while the new cell is given a new ID.

90 DeLTA constructs the lineage tree frame-by-frame, by extending existing cells and creating  
 91 new daughter cells at divisions. However, tracking errors are possible, for example due to  
 92 a temporary air bubble in the field of view, or by a segmentation or a tracking mistake by  
 93 the neural networks. These cases can be corrected by relabeling the cells involved. However,  
 94 relabeling requires updating an entire lineage subtree, an error-prone operation. For this reason,  
 95 we implemented a set of elementary operations on the tree, whose combined effect allows for  
 96 arbitrarily complex lineage tree manipulations [Figure 2].

**Growth rate**



**Figure 3:** Alignment of cell areas for growth rate computation. Circle markers show the logarithm of the area (number of pixels) of a mother cell and two of its daughters. Jumps are where the cell divides. Cross markers show entire cell cycles that are offset (colored arrows) as a function of the relative sizes of the cells after division (highlighted pair of points). The offset is  $\log_2 \left( 1 + \frac{\text{Area}_{\text{mother}}}{\text{Area}_{\text{daughter}}} \right)$ . After offsetting, the growth rate can be computed at any point, even with a centered difference scheme.

Single-cell growth rate is often used as a proxy for cell fitness. Within a given population, individual cells have different growth rates, which can vary with time. The single-cell growth rate,  $\mu(t)$ , satisfies the following differential equation with  $\ell(t)$  the cell length:

$$\frac{d\ell}{dt} = \mu(t)\ell(t)$$

DeLTA can calculate growth rates based on cell area or length. Area-based growth rates rely on direct counts of the number of pixels per cell, while length-based growth rates derive length estimates from the bacterial shape. Growth rates based on volume are not possible to calculate with images at a single focal plane.

Instantaneous growth rate is computed in DeLTA as the derivative of the logarithm of cell length (or area). Because segmentation can make this time series noisy, we use a Savitsky-Golay filter (Savitzky & Golay, 1964) to simultaneously smooth and differentiate the signal. It is a centered finite difference scheme, which is a deliberate choice to avoid discretization biases.

To compute the growth rate, the Savitsky-Golay filter requires at least one data point from the previous frame and one from the next (or more than one for larger window sizes). To avoid apparent jumps in growth rate around cell division events, we offset the areas before and after division by extrapolation of the lineage. This amounts to considering that the area of a mother cell after division is the sum of its own area and that of its daughter [Figure 3].

## <sup>114</sup> File format of results

<sup>115</sup> Analysis results produce image-like data (segmentation masks and label masks), as well as  
<sup>116</sup> scalar data associated with every cell (ID of mother cell), or with every cell and frame (features  
<sup>117</sup> such as length, area, average fluorescence, growth rate). In DeLTA 2.0 we used the pickle  
<sup>118</sup> library to serialize the Python object representing the results into a file. While this allowed  
<sup>119</sup> for saving arbitrary Python objects, these files could only be opened with the same version of  
<sup>120</sup> DeLTA that created them.

<sup>121</sup> In version 3 we now use netCDF4 ([Rew et al., 1989](#)), an open file format based on HDF5  
<sup>122</sup> ([The HDF Group, 2025](#)), popular for storing scientific data with libraries available in many  
<sup>123</sup> programming languages. A limitation of this approach, compared to pickle files, is that the  
<sup>124</sup> HDF5 data format only supports collections of rectangular data arrays, which required us  
<sup>125</sup> to reorganize the data describing cell features and lineages in a rectangular fashion, at the  
<sup>126</sup> expense of file size, although this can be mitigated by compression or by using sparse arrays,  
<sup>127</sup> which is a future goal. The change to netCDF4 is an important improvement for compatibility  
<sup>128</sup> of result files across future versions of DeLTA.

## <sup>129</sup> Conclusion

<sup>130</sup> DeLTA 3.0 enhances function for both novice and experienced users with new features  
<sup>131</sup> (including command-line interface, lineage tree manipulation and growth rate calculation),  
<sup>132</sup> better interoperability (results stored as netCDF files), and backend-agnostic deep-learning  
<sup>133</sup> models (implemented in pure keras).

## <sup>134</sup> Acknowledgements

<sup>135</sup> The authors acknowledge the contributions of Idris Kempf, Caroline Blassick, and Eric Bueno  
<sup>136</sup> to the development of version 3.0 of DeLTA; feedback from the rest of the Dunlop lab; and  
<sup>137</sup> input from the wider community through interactions on DeLTA's gitlab repository.

<sup>138</sup> This work was supported by the National Science Foundation (MCB-2143289) to MJD. VA  
<sup>139</sup> acknowledges support from the European Research Council (ERC-2022-STG, BridgingScales,  
<sup>140</sup> grant agreement 101075989).

<sup>141</sup> As of this version, direct dependencies of DeLTA include numpy ([Harris et al., 2020](#)), scipy  
<sup>142</sup> ([Virtanen et al., 2020](#)), scikit-image ([Walt et al., 2014](#)), xarray ([Hoyer & Hamman, 2017](#)),  
<sup>143</sup> pooch ([Uieda et al., 2020](#)), opencv ([Bradski, 2000](#)), tqdm ([Tqdm/Tqdm, 2025](#)), ffmpeg ([Tomar,  
2006](#)), netCDF4 ([Rew et al., 1989](#)), bioio ([Brown et al., 2023](#)), termcolor ([Termcolor/Termcolor,  
2025](#)), keras ([Chollet & Others, 2015](#)), matplotlib ([Hunter, 2007](#)), and elasticdeform ([Tulder  
& Fringeli, 2024](#)).

<sup>147</sup> Utilities that we use in the development process include ruff ([Astral-Sh/Ruff, 2025](#)), mypy  
<sup>148</sup> ([Python/Mypy, 2025](#)), deptry ([Maas, 2025](#)), pixi ([Arts et al., 2025](#)), pip ([Pypa/Pip,  
2025](#)), pytest ([Krekel et al., 2004](#)), pytest-cov ([Pytest-Dev/Pytest-Cov, 2025](#)), pre-  
<sup>149</sup> commit ([Pre-Commit/Pre-Commit, 2025](#)), sphinx ([Sphinx-Doc/Sphinx, 2025](#)), numpydoc  
<sup>150</sup> ([Numpy/Numpydoc, 2025](#)), sphinx-design ([Executablebooks/Sphinx-Design, 2025](#)), and furo  
<sup>151</sup> ([Gedam, 2025](#)).

## <sup>153</sup> AI Usage Disclosure

<sup>154</sup> No generative AI was used in the software creation, documentation, or paper authoring.

## 155 References

- 156 Abadi, M., Agarwal, A., Barham, P., Brevdo, E., Chen, Z., Citro, C., Corrado, G. S., Davis,  
157 A., Dean, J., Devin, M., Ghemawat, S., Goodfellow, I., Harp, A., Irving, G., Isard, M.,  
158 Jozefowicz, R., Jia, Y., Kaiser, L., Kudlur, M., ... Zheng, X. (2015). *TensorFlow: Large-scale  
159 machine learning on heterogeneous systems*. <https://doi.org/10.5281/zenodo.4724125>
- 160 Ahmadi, A., Courtney, M., Ren, C., & Ingalls, B. (2024). A benchmarked comparison  
161 of software packages for time-lapse image processing of monolayer bacterial population  
162 dynamics. *Microbiology Spectrum*. <https://doi.org/10.1128/spectrum.00032-24>
- 163 Allard, P., Papazotos, F., & Potvin-Trottier, L. (2022). Microfluidics for long-term single-  
164 cell time-lapse microscopy: Advances and applications. *Frontiers in Bioengineering and  
165 Biotechnology*, 10. <https://doi.org/10.3389/fbioe.2022.968342>
- 166 Ansel, J., Yang, E., He, H., Gimelshein, N., Jain, A., Voznesensky, M., Bao, B., Bell, P.,  
167 Berard, D., Burovski, E., Chauhan, G., Chourdia, A., Constable, W., Desmaison, A.,  
168 DeVito, Z., Ellison, E., Feng, W., Gong, J., Gschwind, M., ... Chintala, S. (2024, April).  
169 PyTorch 2: Faster Machine Learning Through Dynamic Python Bytecode Transformation  
170 and Graph Compilation. *29th ACM International Conference on Architectural Support  
171 for Programming Languages and Operating Systems, Volume 2 (ASPLOS '24)*. <https://doi.org/10.1145/3620665.3640366>
- 172 Arts, R., Zalmstra, B., Vollprecht, W., Jager, T. de, Morcotoilo, N., & Hofer, J. (2025). *Pixi*.  
173 <https://github.com/prefix-dev/pixi/releases/tag/v0.53.0>
- 174 175 *Astral-sh/ruff*. (2025). Astral. <https://github.com/astral-sh/ruff>
- 176 Bradbury, J., Frostig, R., Hawkins, P., Johnson, M. J., Leary, C., Maclaurin, D., Necula, G.,  
177 Paszke, A., VanderPlas, J., Wanderman-Milne, S., & Zhang, Q. (2018). *JAX: Composable  
178 transformations of Python+NumPy programs* (Version 0.3.13). [http://github.com/jax-  
ml/jax](http://github.com/jax-<br/>179 ml/jax)
- 180 Bradski, G. (2000). The OpenCV library. *Dr. Dobb's Journal of Software Tools*.
- 181 Brown, E. M., Toloudis, D., Sherman, J., Swain-Bowden, M., Lambert, T., Meharry, S.,  
182 Whitney, B., & BioIO Contributors. (2023). *BioIO: Image reading, metadata conversion,  
183 and image writing for microscopy images in pure python*. GitHub. [https://github.com/bioio-  
devs/bioio](https://github.com/bioio-<br/>184 devs/bioio)
- 185 Chollet, F., & Others. (2015). *Keras*. <https://keras.io>
- 186 Cutler, K. J., Stringer, C., Lo, T. W., Rappez, L., Stroustrup, N., Brook Peterson, S.,  
187 Wiggins, P. A., & Mougous, J. D. (2022). Omnipose: A high-precision morphology-  
188 independent solution for bacterial cell segmentation. *Nature Methods*, 19(11), 1438–1448.  
189 <https://doi.org/10.1038/s41592-022-01639-4>
- 190 Executablebooks/sphinx-design. (2025). Executable Books. [https://github.com/  
executablebooks/sphinx-design](https://github.com/<br/>191 executablebooks/sphinx-design)
- 192 Gedam, P. (2025). *Pradyunsg/furo*. <https://github.com/pradyunsg/furo>
- 193 Gericke, B., Degner, F., Hüttmann, T., Werth, S., & Fortmann-Grote, C. (2025). *Performance  
194 review of retraining and transfer learning of DeLTA2 for image segmentation for  
195 pseudomonas fluorescens SBW25*. 273–280. ISBN: 978-989-758-688-0
- 196 Harris, C. R., Millman, K. J., Walt, S. J. van der, Gommers, R., Virtanen, P., Cournapeau, D.,  
197 Wieser, E., Taylor, J., Berg, S., Smith, N. J., Kern, R., Picus, M., Hoyer, S., Kerkwijk,  
198 M. H. van, Brett, M., Haldane, A., Río, J. F. del, Wiebe, M., Peterson, P., ... Oliphant,  
199 T. E. (2020). Array programming with NumPy. *Nature*, 585(7825), 357–362. <https://doi.org/10.1038/s41586-020-2649-2>

- 201 Hoyer, S., & Hamman, J. (2017). Xarray: N-d labeled arrays and datasets in python. *Journal  
202 of Open Research Software*, 5(1). <https://doi.org/10.5334/jors.148>
- 203 Hunter, J. D. (2007). Matplotlib: A 2D graphics environment. *Computing in Science &  
204 Engineering*, 9(3), 90–95. <https://doi.org/10.1109/MCSE.2007.55>
- 205 Krekel, H., Oliveira, B., Pfannschmidt, R., Bruynooghe, F., Laugher, B., & Bruhin, F. (2004).  
206 Pytest 7.5 (Version 7.5). <https://github.com/pytest-dev/pytest>
- 207 Lugagne, J.-B., Lin, H., & Dunlop, M. J. (2020). DeLTA: Automated cell segmentation,  
208 tracking, and lineage reconstruction using deep learning. *PLOS Computational Biology*,  
209 16(4), e1007673. <https://doi.org/10.1371/journal.pcbi.1007673>
- 210 Maas, F. (2025). *Fpgmaas/deptr*. <https://github.com/fpgmaas/deptr>
- 211 Numpy/numpydoc. (2025). NumPy. <https://github.com/numpy/numpydoc>
- 212 O'Connor, O. M., Alnahhas, R. N., Lugagne, J.-B., & Dunlop, M. J. (2022). DeLTA 2.0: A  
213 deep learning pipeline for quantifying single-cell spatial and temporal dynamics. *PLOS  
214 Computational Biology*, 18(1), e1009797. <https://doi.org/10.1371/journal.pcbi.1009797>
- 215 O'Connor, O. M., & Dunlop, M. J. (2025). Cell-TRACTR: A transformer-based model for  
216 end-to-end segmentation and tracking of cells. *PLOS Computational Biology*, 21(5),  
217 e1013071. <https://doi.org/10.1371/journal.pcbi.1013071>
- 218 Perez, F., Granger, B. E., & Hunter, J. D. (2011). Python: An ecosystem for scientific  
219 computing. *Computing in Science & Engineering*, 13(2), 13–21. [https://doi.org/10.1109/MCSE.2010.119](https://doi.org/10.1109/<br/>220 MCSE.2010.119)
- 221 Pre-commit/pre-commit. (2025). pre-commit. <https://github.com/pre-commit/pre-commit>
- 222 Pypa/pip. (2025). Python Packaging Authority. <https://github.com/pypa/pip>
- 223 Pytest-dev/pytest-cov. (2025). pytest-dev. <https://github.com/pytest-dev/pytest-cov>
- 224 Python/mypy. (2025). Python. <https://github.com/python/mypy>
- 225 Rew, R., Davis, G., Emmerson, S., Cormack, C., Caron, J., Pincus, R., Hartnett, E., Heimbigner,  
226 D., Appel, L., & Fisher, W. (1989). Unidata NetCDF. UCAR/NCAR - Unidata. <https://doi.org/10.5065/D6H70CW6>
- 228 Ronneberger, O., Fischer, P., & Brox, T. (2015). U-net: Convolutional networks for biomedical  
229 image segmentation. In N. Navab, J. Hornegger, W. M. Wells, & A. F. Frangi (Eds.),  
230 *Medical image computing and computer-assisted intervention – MICCAI 2015* (Vol. 9351,  
231 pp. 234–241). Springer International Publishing. [https://doi.org/10.1007/978-3-319-24574-4\\_28](https://doi.org/10.1007/978-3-319-<br/>232 24574-4_28)
- 233 Savitzky, Abraham., & Golay, M. J. E. (1964). Smoothing and differentiation of data by  
234 simplified least squares procedures. *Analytical Chemistry*, 36(8), 1627–1639. <https://doi.org/10.1021/ac60214a047>
- 236 Sphinx-doc/sphinx. (2025). Sphinx. <https://github.com/sphinx-doc/sphinx>
- 237 Stewart, E. J., Madden, R., Paul, G., & Taddei, F. (2005). Aging and death in an organism  
238 that reproduces by morphologically symmetric division. *PLOS Biology*, 3(2), e45. <https://doi.org/10.1371/journal.pbio.0030045>
- 240 Stirling, D. R., Swain-Bowden, M. J., Lucas, A. M., Carpenter, A. E., Cimini, B. A., &  
241 Goodman, A. (2021). CellProfiler 4: Improvements in speed, utility and usability. *BMC  
242 Bioinformatics*, 22(1), 1–11. <https://doi.org/10.1186/s12859-021-04344-9>
- 243 Stringer, C., Wang, T., Michaelos, M., & Pachitariu, M. (2021). Cellpose: A generalist  
244 algorithm for cellular segmentation. *Nature Methods*, 18(1), 100–106. <https://doi.org/10.1038/s41592-020-01018-x>

- 246 *Termcolor/termcolor*. (2025). termcolor. <https://github.com/termcolor/termcolor>
- 247 The HDF Group. (2025). *Hierarchical data format, version 5*. <https://github.com/HDFGroup/hdf5>
- 249 Thiermann, R., Sandler, M., Ahir, G., Sauls, J. T., Schroeder, J., Brown, S., Le Treut, G.,  
250 Si, F., Li, D., Wang, J. D., & Jun, S. (2024). Tools and methods for high-throughput  
251 single-cell imaging with the mother machine. *eLife*, 12, RP88463. <https://doi.org/10.7554/eLife.88463>
- 253 Tomar, S. (2006). Converting video formats with FFmpeg. *Linux J.*, 2006(146), 10.
- 254 *Tqdm/tqdm*. (2025). tqdm developers. <https://github.com/tqdm/tqdm>
- 255 Tulder, G. van, & Fringeli, G. (2024). *Gvtulder/elasticdeform: Version v0.5.1*. Zenodo.  
256 <https://doi.org/10.5281/zenodo.11267397>
- 257 Uieda, L., Soler, S. R., Rampin, R., Kemenade, H. van, Turk, M., Shapero, D., Banahirwe, A.,  
258 & Leeman, J. (2020). Pooch: A friend to fetch your data files. *Journal of Open Source  
Software*, 5(45), 1943. <https://doi.org/10.21105/joss.01943>
- 260 Valen, D. A. V., Kudo, T., Lane, K. M., Macklin, D. N., Quach, N. T., DeFelice, M. M.,  
261 Maayan, I., Tanouchi, Y., Ashley, E. A., & Covert, M. W. (2016). Deep learning  
262 automates the quantitative analysis of individual cells in live-cell imaging experiments. *PLOS  
Computational Biology*, 12(11), e1005177. <https://doi.org/10.1371/journal.pcbi.1005177>
- 264 Virtanen, P., Gommers, R., Oliphant, T. E., Haberland, M., Reddy, T., Cournapeau, D.,  
265 Burovski, E., Peterson, P., Weckesser, W., Bright, J., Walt, S. J. van der, Brett, M.,  
266 Wilson, J., Millman, K. J., Mayorov, N., Nelson, A. R. J., Jones, E., Kern, R., Larson, E.,  
267 ... Mulbregt, P. van. (2020). SciPy 1.0: Fundamental algorithms for scientific computing  
268 in python. *Nature Methods*, 17(3), 261–272. <https://doi.org/10.1038/s41592-019-0686-2>
- 269 Walt, S. van der, Schönberger, J. L., Nunez-Iglesias, J., Boulogne, F., Warner, J. D., Yager,  
270 N., Gouillart, E., & Yu, T. (2014). Scikit-image: Image processing in python. *PeerJ*, 2,  
271 e453. <https://doi.org/10.7717/peerj.453>
- 272 Wang, P., Robert, L., Pelletier, J., Dang, W. L., Taddei, F., Wright, A., & Jun, S. (2010).  
273 Robust growth of escherichia coli. *Current Biology*, 20(12), 1099–1103. <https://doi.org/10.1016/j.cub.2010.04.045>
- 274